



This document was prepared for the ETI by third parties under contract to the ETI. The ETI is making these documents and data available to the public to inform the debate on low carbon energy innovation and deployment.

Programme Area: Marine

Project: PerAWAT

Title: GH Far Wake Modelling Report

Abstract:

This document outlines the issues associated with modelling the far wake region within an array of tidal turbines. A review of the existing literature is presented which provides an overview of both the applicable modelling options which characterise the wake region of interest. The GH far wake model is described and the modelling approach justified. The GH far wake model simplifies the fundamental Navier-Stokes equations to allow a computationally efficient method to evaluate far wake development. To account for any surrounding bounding effects a hybrid method is used. The model is initialised by the GH device scale models and then the solution propagates downstream. The key parameters which affect the model include: the ambient flow turbulence and the potential impact of bounding surfaces and/or other surrounding turbines. Wake merging models are used to combine multiple wakes. Flow diagrams of the GH far wake model algorithms are presented. Existing validation of the aspects of the modelling method are presented.

Context:

The Performance Assessment of Wave and Tidal Array Systems (PerAWaT) project, launched in October 2009 with £8m of ETI investment. The project delivered validated, commercial software tools capable of significantly reducing the levels of uncertainty associated with predicting the energy yield of major wave and tidal stream energy arrays. It also produced information that will help reduce commercial risk of future large scale wave and tidal array developments.

Disclaimer:

The Energy Technologies Institute is making this document available to use under the Energy Technologies Institute Open Licence for Materials. Please refer to the Energy Technologies Institute website for the terms and conditions of this licence. The Information is licensed 'as is' and the Energy Technologies Institute excludes all representations, warranties, obligations and liabilities in relation to the Information to the maximum extent permitted by law. The Energy Technologies Institute is not liable for any errors or omissions in the Information and shall not be liable for any loss, injury or damage of any kind caused by its use. This exclusion of liability includes, but is not limited to, any direct, indirect, special, incidental, consequential, punitive, or exemplary damages in each case such as loss of revenue, data, anticipated profits, and lost business. The Energy Technologies Institute does not guarantee the continued supply of the Information. Notwithstanding any statement to the contrary contained on the face of this document, the Energy Technologies Institute confirms that the authors of the document have consented to its publication by the Energy Technologies Institute.

**ETI MARINE PROGRAMME PROJECT
PERAWAT MA1003
WG3WP4 D5 GH FAR WAKE
MODELLING REPORT**

Client	Energy Technologies Institute
Contact	Geraldine Newton-Cross
Document No	104329/BR/05
Issue	2.0
Classification	Not to be disclosed other than in line with the terms of the Technology Contract
Date	3 rd March 2011

Author: M D Thomson/L Gill/R Collings

Checked by: J I Whelan

Approved by: R I Rawlinson-Smith

IMPORTANT NOTICE AND DISCLAIMER

1. This report (“Report”) is prepared and issued by Garrad Hassan & Partners Ltd (“GH” or “Garrad Hassan”) for the sole use of the client named on its title page (the “Client”) on whose instructions it has been prepared, and who has entered into a written agreement directly with Garrad Hassan. Garrad Hassan’s liability to the Client is set out in that agreement. Garrad Hassan shall have no liability to third parties (being persons other than the Client) in connection with this Report or for any use whatsoever by third parties of this Report unless the subject of a written agreement between Garrad Hassan and such third party. The Report may only be reproduced and circulated in accordance with the Document Classification and associated conditions stipulated or referred to in this Report and/or in Garrad Hassan’s written agreement with the Client. No part of this Report may be disclosed in any public offering memorandum, prospectus or stock exchange listing, circular or announcement without the express written consent of Garrad Hassan. A Document Classification permitting the Client to redistribute this Report shall not thereby imply that Garrad Hassan has any liability to any recipient other than the Client.
2. This report has been produced from information relating to dates and periods referred to in this report. The report does not imply that any information is not subject to change.

KEY TO DOCUMENT CLASSIFICATION

Strictly Confidential	:	For disclosure only to named individuals within the Client’s organisation.
Private and Confidential	:	For disclosure only to individuals directly concerned with the subject matter of the Report within the Client’s organisation.
Commercial in Confidence	:	Not to be disclosed outside the Client’s organisation
GH only	:	Not to be disclosed to non GH staff
Client’s Discretion	:	Distribution for information only at the discretion of the Client (subject to the above Important Notice and Disclaimer).
Published	:	Available for information only to the general public (subject to the above Important Notice and Disclaimer and Disclaimer).

REVISION HISTORY

Issue	Issue date	Summary
1.0	21/12/10	Original issue (electronic version only)
2.0	03/03/11	Second release, revised according to ETI feedback (electronic copy only)

CONTENTS

EXECUTIVE SUMMARY	1
SUMMARY OF NOTATION	2
1 INTRODUCTION	3
1.1 Scope of this document	3
1.2 Purpose of this document	3
1.3 Specific tasks associated with WG3 WP4 D5	3
1.4 WG3 WP4 D5 acceptance criteria	3
2 BACKGROUND	4
2.1 Properties of a tidal wake	4
2.2 Comparison with between wind and tidal turbine wakes	5
2.3 Factors affecting the far wake of a tidal turbine	7
2.4 Ducted and open-centre turbines	8
3 REVIEW OF RELEVANT MODELLING METHODOLOGIES	9
3.1 Kinematic Models	9
3.2 3-d Potential Flow Theory	10
3.3 Simplified Computational Fluid Dynamics (CFD) Models	10
3.4 CFD models (Navier-Stokes solvers)	11
3.5 Added turbulence intensity modelling	12
3.6 Array Modelling	12
3.7 Summary of relevant modelling methods	13
3.8 Review of relevant experimental work	14
4 THE GH FAR WAKE MODEL	15
4.1 GH modelling philosophy	15
4.2 Description of the GH far wake model	15
5 GH FAR WAKE MODEL THEORY	17
5.1 The Eddy Viscosity wake model	17
5.2 Momentum integral model	20
5.3 Wake interaction models	21
5.4 Semi-empirical added turbulence intensity model	22
5.5 Summary of the key assumptions	22
6 GH FAR WAKE MODEL METHODOLOGY AND IMPLEMENTATION	23
6.1 Far wake modelling	24
6.2 Implementation	26
7 VALIDATION	28
7.1 Existing verification and validation GH far wake model	28

7.2	Developments under PerAWaT	36
8	SUMMARY	37
9	BIBLIOGRAPHY	38

LIST OF TABLES

Table 2-1: Numerical comparison of tidal and wind turbine parameters 6

Table 3-1: Summary table comparing modelling methodologies 13

Table 5-1 : Wake merging models 21

Table 6-1 Summary functional description 27

Table 6-2 Detailed functional description of the far wake model 27

LIST OF FIGURES

Figure 3-1: CFD representation of a tidal turbine array layout from above. Reproduced from Bai et al. (2009) 12

Figure 5-1: Wake profile used in the eddy viscosity model 18

Figure 5-2: Elliptical Gaussian wake model 20

Figure 6-1: Hierarchy of modelling domains and scales 23

Figure 6-2: Overview of TidalFarmer software architecture showing the GH Wake routine in its context 23

Figure 6-3 Flow diagram of the GH Far wake modelling 25

Figure 6-4: Flow diagram of the GH eddy-viscosity wake model 26

Figure 7-1 Visualisation of the flow field behind a porous disc in a boundless flow (top: slice through the depth at the wake centreline, bottom: slice across the water column at the wake centreline)..... 29

Figure 7-2 Profile plots of the lateral and vertical Reynolds Stresses at different locations downstream of a porous disc in a boundless flow 30

Figure 7-3 Matching the eddy-viscosity model to measured data 31

Figure 7-4 Comparison of the split model solutions, the combined model solution and measure data (where the porous disc sits 1/3 of the water depth from the flume floor) 32

Figure 7-5 Comparison of a Gaussian profile compared to measured data points (left: depth profiles, right: lateral profile, dimensions in rotor diameters)..... 32

Figure 7-6 Visualisation of measured wake data with an elliptical Gaussian fit (the wake is bounded by a free surface and seabed at +/-1.25D); the colour bar indicates the velocity deficit..... 34

Figure 7-7: Illustrations of the far wake added turbulence intensity model and comparison with rotor wake data 35

EXECUTIVE SUMMARY

This document outlines the issues associated with modelling the far wake region within an array of tidal turbines. A review of the existing literature is presented which provides an overview of both the applicable modelling options which characterise the wake region of interest. The GH far wake model is described and the modelling approach justified.

The GH far wake model simplifies the fundamental Navier-Stokes equations to allow a computationally efficient method to evaluate far wake development. To account for any surrounding bounding effects a hybrid method is used. The model is initialised by the GH device scale models and then the solution propagates downstream. The key parameters which affect the model include: the ambient flow turbulence and the potential impact of bounding surfaces and/or other surrounding turbines. Wake merging models are used to combine multiple wakes.

The GH far wake modelling theory is described and the method by which the mathematical models are implemented into a working code is described, as is the way in which the GH far wake model is to be incorporated within the GH TidalFarmer Beta code. Flow diagrams of the GH far wake model algorithms are presented.

Existing validation of the aspects of the modelling method are presented. However, one of the main aims of the PerAWaT project is to robustly evaluate the appropriateness of using the adapted axi-symmetric far wake model to represent the wake behind an array of tidal turbine.

The PerAWaT work packages WG4WP1 & WG4WP3 will provide information regarding the development of a single bounded wake (the latter focusing on ducted and open centre concepts). The experiments planned in WG4WP2 will provide data informing on the impact of the changes in ambient flow conditions, bounding effect of a free surface and seabed, as well as the selection of the most appropriate wake merging models.

SUMMARY OF NOTATION

Turbine characteristics

D Rotor diameter

Wake Field

B_w Wake width
 B_{wy} Horizontal wake width
 B_{wz} Vertical wake width
 D_m Centreline velocity deficit
 I_{amb} Ambient turbulent intensity
 L_m Length scale of turbulence
 M Linear momentum deficit
 U_m Velocity scale of turbulence
 ε Overall eddy viscosity
 ε_{amb} Ambient eddy viscosity

U Axial flow velocity
 V Radial flow velocity
 U_{def} Total velocity deficit in wake
 U_c Wake centreline axial flow velocity
 U_i Incident axial flow speed on rotor
 U_o Mean free stream axial flow speed
 x_n Length of the near wake

Constants

ρ Density
 μ Dynamic viscosity
 ν Kinematic viscosity
 g Gravitational acceleration
 K_K Von Karman constant

Cylindrical Co-ordinate systems

x Axial co-ordinate
 r Radial co-ordinate

Abbreviations

1-d one dimension (typically in the x-direction)
 2-d two dimensions
 3-d three dimensions

CFD Computational fluid dynamics
 FDC Fundamental Device Concepts
 RANS Reynolds averaged Navier-Stokes

A general glossary on tidal energy terms was provided as part of WG0 D2 – “Glossary of PerAWaT terms”. This is a working document which will be revised as the project progresses.

1 INTRODUCTION

1.1 Scope of this document

This document constitutes the fifth deliverable (D5) of working group 3, work package 4 (WG3WP4) of the PerAWaT (Performance Assessment of Wave and Tidal Arrays) project funded by the Energy Technologies Institute (ETI). Garrad Hassan and Partners Ltd (GH) is the sole contributor to this work package. This document describes the theory behind and the method of implementation of the mathematical models used to evaluate the far wake forms behind a tidal turbine.

1.2 Purpose of this document

The purpose of WG3WP4 is to develop, validate and document an engineering tool that allows a rapid assessment of the energy yield potential of a tidal turbine array on non-specialist hardware. The specific objective of WG3 WP4 D5 is to both document and provide a technical justification for the use of the existing GH far wake model within the suite of models that make up the engineering tool ‘TidalFarmer’.

1.3 Specific tasks associated with WG3 WP4 D5

WG3WP4 D5 comprises the following aspects:

- A detailed description of the theoretical basis of the GH far wake model
- A description of modelling methodology
- A description of the method of integrating the GH far wake model into the GH complete engineering tool code

1.4 WG3 WP4 D5 acceptance criteria

The acceptance criteria as stated in Schedule five of the PerAWaT technology contract are as follows:

D5: Far wake modelling report describes:

- How the existing GH far wake model has been extended to incorporate turbulence intensities and multiple wake interactions
- The theory and methodology (assumptions and algorithms) behind the resulting far wake model
- The method of integrating this model within the Beta code

2 BACKGROUND

In this section, the concept of a wake is first presented, and a comparison between tidal and wind turbine wakes is made (repeated from the near wake report (WG3WP4 D2)). Factors which particularly affect the far wake are then discussed, and the section concludes with a brief look at how the far wake may be different for ducted and open-centre turbines. A detailed discussion of the various regions and profiles found in wakes is presented in Section 2.3 of the near wake report (WG3WP4 D2).

2.1 Properties of a tidal wake

Downstream of a tidal turbine a turbulent wake region is formed, in which the mean velocity is lower than that of the surrounding fluid. For modelling purposes, this is typically divided into three regions. The near wake is immediately downstream of the rotor, where flow in the region is highly dependent on exact rotor characteristics. A turbulent shear layer forms between the slower moving wake fluid and the ambient flow. This layer thickens with downstream distance until it meets the wake centreline and the near wake region ends. A short transition region exists before the far wake region is said to have begun, as shown in the Figure 2.4 below.

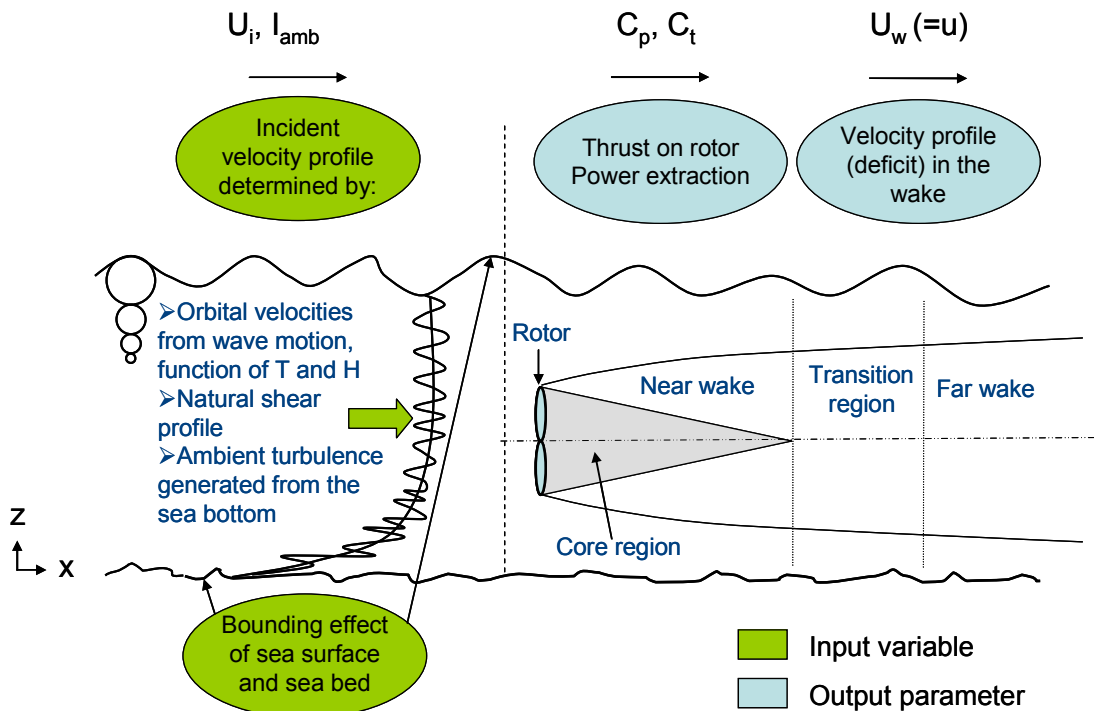


Figure 2.4 Illustration of the beginning of the far wake region (and including variables affecting device performance and wake structure).

The far wake structure is influenced through two key mechanisms. Convection drives the flow, and turbulent mixing with ambient flow re-energises the wake, increasing the velocity until it is similar to the freestream velocity at a point far downstream. Throughout the far wake, the velocity deficit profile approximately follows a Gaussian distribution.

2.2 Comparison with between wind and tidal turbine wakes

The flow through and around a tidal turbine has many similarities with other commonly found rotors, in particular wind turbines. As for a wind turbine, the kinetic energy of the fluid (tidal stream) is converted into the rotational energy of the turbine, simultaneously driving a generator and thus creating electric power. Thake (2005) has shown that power performance of Marine Current Turbines' "SeaFlow" device (a 300kW prototype) demonstrates reasonable agreement with predictions from a blade element momentum (BEM) code. BEM codes are the design and prediction method that is used predominantly in the wind energy industry. This provides anecdotal evidence that process of energy (or momentum) extraction is very similar to that which is understood for wind turbines.

However there are some key differences between the flows that wind and tidal turbines operate in, these include:

- the presence of a bounding free surface (leading to blockage)
- additional types of flow unsteadiness (such as due to the effect of passing waves and different types of turbulence)

Cavitation is an added dynamic effect that has the potential to occur on parts of tidal turbines but is not a factor for consideration on wind turbines. However since cavitation will only have an indirect impact on the wake structure and since the majority (if not all) device developers are likely to design their devices to avoid the occurrence of cavitation, due to its adverse impacts, it will not be considered further in this report.

There is also a concern that tidal flow turbulence characteristics may be shown to be site-specific, and thus be difficult to describe using standardised turbulence models, as discussed in the BERR report prepared by GH (2008). The differences between the flow environments that wind and tidal turbines operate within will lead to differences in the specific wake form and its evolution and these are discussed further in Section 2.3. Table 2-1 summarises the main parameters which characterise the flow environment and performance measurements of tidal and wind turbines.

Table 2-1: Numerical comparison of tidal and wind turbine parameters

Global constants		Air ¹	Water ¹		Ratio A/W
Gravitational acceleration	g	9.81	9.81	m/s ²	1.00
Density	ρ	1.225	1000	kg/m ³	0.0012
Dynamic viscosity	μ	1.79E-05	1.14E-03	kg/ms	0.016
Kinematic viscosity	ν	1.46E-05	1.14E-06	m/s	12.38
Environment					
typical rating velo (hh)	U_o	12.0	2.7	m/s	4.51
typical mean velo		10	1.5	m/s	6.67
typical extreme		70	4.5	m/s	15.56
ratio mean to extreme		7	3		2.33
ratio rated to extreme		5.8	1.7		3.45
boundary layer					
height to free stream flow		2,000	44		
Re BL		4.59E+07	5.03E+07		0.91
typical roughness (sand)		0.0003	0.0003		
typical power law (sand)		0.1000	0.1429		
angle of slope for separation		<17'			
Typical characteristics for a 1MW device					
Turbine diameter (length-scale)	D	50	18	m	2.78
Swept area	A	1963	254	m ²	7.72
Thrust coefficient	C_t	0.89	0.89		1.00
Power coefficient	C_p	0.5	0.45		1.11
Rated power electrical	P_e	1.00	1.00	MW	1.00
Rated power mechanical	P	1.10	1.10	MW	1.00
Rated thrust	T	163	735	kN	0.22
Rated power to thrust ratio	P/T	6.7	1.5		4.50
Rated impedance (T/ U_o)	Im	13,623	276,234	kg/s	0.05
Rated momentum flux		93	3,610	kg /ms ²	0.03
Typical hub height		50	20		
Peak steady tower bending moment		8169	14699	kNm	0.56

As shown in Table 2-1 below at a typical rated flow speed (where the steady axial thrust is typically at a maximum) the power to axial thrust ratio is almost five times higher for the wind turbine than a tidal turbine (assuming the same power and thrust coefficients to equivalently rated wind and tidal turbines designed to generate that power for speeds of 12m/s and 2.7m/s respectively). Hence the forces experienced by a tidal turbine per unit radial span are going to be significantly higher than the equivalent forces experienced by a wind turbine for the majority of its working life-span. As a consequence modifications will be required to the structural design of the rotor blades compared with wind turbines, i.e. they will have a higher solidity and a thicker chord distribution. This will impact on the specific form of the near wake.

However, the ratio between the momentum deficit compared to the influx momentum in a tidal turbine wake is characterised by the thrust coefficient. Leading device developers such as TGL, MCT and Hammerfest Strøm all report similar thrust coefficients to wind turbines. Some device developers are pursuing different operating philosophies such as stall regulated

¹ Conditions at 15°C and 101.3 kN/m². NB. Values for sea water will be slightly altered due to salinity.

or over-speed operation (or even rating at the peak flow speed), which is in contrast to the more-or-less wind industry standard operating philosophy of pitch regulation.

It is the study of the impact of the bounding surfaces and flow unsteadiness on wake recovery lengths, and hence array layouts, that comprises a major part of the PerAWaT project. The effect of the turbulent wake on downstream devices is highly significant. In the wind industry, a reduction in velocity of no more than 10% is typically to be tolerated for downstream turbines, equating to a power reduction of almost 30% due to the relationship of power to velocity cubed. Beyond this level the losses become unacceptable. For wind turbines, this results in a device spacing of 5 to 10 rotor diameters in the predominant flow direction.

2.3 Factors affecting the far wake of a tidal turbine

The main factors which will affect the far wake of a tidal-stream turbine are:

- Initial conditions – velocity deficit and added turbulence induced by the turbine
- Support structure/foundation effect.
- The ambient turbulence intensity
- Proximity to bounding surfaces such as the free-surface or seabed.
- Proximity to other devices (lateral and longitudinal)

The potential effects of these parameters are detailed in this section.

Within the far wake, the velocity is largely independent of exact turbine geometry (Crespo et al. (1999)). The turbine geometry (e.g. number of blades, load distribution, hub size) impacts the near wake, but the far wake is defined as the point where the shear layers meet the wake centreline, and at this point the wake has developed into a bell shape similar to a Gaussian profile (Lissaman (1979)). In the hypothetical situation in which no ambient shear layer or bounding surface is present, the far wake can be assumed to be axi-symmetric with self-similar velocity profiles throughout. Only two parameters contribute to the approximately Gaussian initial velocity profile, namely the thrust on the turbine and total turbulence kinetic energy produced by the rotor. Although the complex rotor geometry does not directly affect the far wake, its influence is parameterised for the analysis of the far wake as a velocity deficit and added turbulence intensity.

As the wake propagates downstream, momentum is transferred into the wake through turbulent mixing with the ambient flow, reducing the velocity deficit until it approaches that of the free stream. Once into the far wake region, this recovery process is driven primarily by the ambient turbulence, which can significantly enhance the mixing process and hence accelerate the re-energising of the wake. Ambient turbulence intensity is prominently governed by the seabed roughness, but can also be affected by free-surface waves. Certain wave states and operating depths may significantly impact on the entire wake recovery process.

The presence of a boundary layer (shear profile) at tidal energy sites invalidates the earlier assumption of axial-symmetry in the wake. There is little data on the general form of the boundary layer, but the available data sets to-date suggests wide variations from sites to site. Operating in the lower region of the boundary layer may lead to a significant asymmetry in the flow above and below the wake, altering the velocity profile and the recovery of the wake. Through the testing of mesh disks in a tidal flume, Myers et al. (2010) have shown a significant increase in the recovery distance when in close proximity to a bounding surface. A 10cm disc centred 10cm above the bed of the flume showed a centreline velocity deficit of approximately 14% at 20 rotor diameters downstream. This compares to a deficit of approximately 7% for the same disc centred 20cm from the bottom surface. The authors

postulated that a restriction of the mass flow rate underneath the disc leads to a slow-moving region of flow underneath the wake, insufficient to re-energise it from below.

As explained in detail in Section 6, the primary objective of the GH far wake model is to evaluate the wake propagation of individual turbines within an array, anticipating wake interaction and the impact of one device upon another. Hence the investigation of wake propagation and evolution within an array under different flow environments and array configurations forms a major objective of the PerAWaT project.

2.4 Ducted and open-centre turbines

The unducted 3-bladed horizontal rotor has emerged as the leading technology in the wind energy sector. Tidal stream energy conversion technology is at a very early stage of development and at present there are a multitude of different technological approaches towards capturing tidal stream energy. More detail on the different fundamental device concepts (FDCs) currently being pursued has been provided in WG0 D2. Within the PerAWaT project three fundamental rotor configurations have been selected for analysis:

- Three bladed horizontal axis axial flow turbine (three bladed turbine)
- Ducted horizontal axis axial flow turbine (ducted turbine)
- Open-centre horizontal axis axial flow turbine (open-centre turbine)

Literature on the form of the far wake for either ducted or open-centre horizontal axis axial flow turbines is scarce. Although the configuration of the turbine is likely to have a significant effect on the near wake, it is expected that the far wake of each would be similar and converge towards an approximately Gaussian velocity profile.

Aspects of the numerical simulations and experiments being conducted as part of WG3WP1, WG3WP5, WG4WP1 and WG4WP3 will enable any differences in the far wake region between the rotor configurations described above to be identified and assessed.

3 REVIEW OF RELEVANT MODELLING METHODOLOGIES

To date research into tidal turbine-specific effects, such as a bounding free surface and seabed and different ambient flow conditions, has been limited. However a review of the literature reveals an extensive body of theory on wake modelling methodologies which can be adopted from the wind energy sector (see Section 2.2). In particular there has been a large focus on far wake modelling, due to the impact of lower velocity and higher turbulence incident on downstream devices. Work on wind turbine wakes has led to models with varying degrees of sophistication. Complex field models at one end of the spectrum attempt to model the wake using the fundamental equations of motion, whereas at the other end of the spectrum empirical approximations are used in kinematic models to describe the wake. For the purposes of this report the relevant wake modelling methodologies are divided into four categories:

- Kinematic Models
- 3-d Potential Flow Theory
- Simplified Computational Fluid Dynamics (CFD) Models
- CFD Models (Navier-Stokes solvers)

It must be noted that not all models fit exactly within a single category, and there is some degree of overlap. Review papers by Crespo et al. (1999) and Vermeer et al. (2003) provide a comprehensive summary of the existing modelling methods for wind turbine wakes and present the fundamental equations upon which each method is based. This section presents an overview of these modelling methodologies, each with varying computational requirements. The reader is directed to the publications by Crespo and Vermeer for more specific detail on these methodologies.

Traditionally, far wake research has been more focused on array effects, while the near wake research has been primarily focused on assessment of performance and loading on a single wind turbine. Because the near wake characteristics of the flow are initial conditions for the far wake, reference to the near wake in the work on the far wake is often made, and vice versa, hence it is difficult to draw an exact distinction between the methodologies employed for the near and far wake research.

3.1 Kinematic Models

The first approach to wake modelling was that introduced in a seminal paper by Lissaman (1979), who described the model as kinematic. Such models make use of self-similar velocity profiles obtained from experimental and theoretical work on co-flowing jets. Each of the three primary wake regions is typically represented using a different profile. Lissaman selected a box shaped profile (often referred to as a “top-hat”) for the near wake, a blunt bell shape for the transition region and a bell shape similar to a Gaussian profile for the far wake.

The majority of kinematic models calculate an initial velocity from global momentum conservation, with the thrust coefficient of the turbine as an input. In Lissaman’s model, wake growth is given by the sum of ambient turbulence and the turbulence resulting from shear in the wake. The ground effect is simulated using imaging techniques.

The Jensen model by Katic et al. (1986) is even more simplified, assuming a top-hat shaped velocity deficit throughout the entire wake. The wake radius is assumed to grow linearly with downstream distance, allowing the velocity deficit and width to be found at any downstream

distance without the need to calculate the previous values. Despite the significant discrepancies with measurements in the near wake region due to the model's rectangular distribution, the momentum extracted is surprisingly accurate. The model therefore provides a simple, but accurate, calculation of energy output. For this reason the Jensen model is commonly adopted in commercial codes which require a large number of calculations, for example wind farm analysis codes requiring computation of a large number of different flow directions.

3.2 3-d Potential Flow Theory

Potential flow methods idealise the fluid to allow analytical solutions of the flow field around a body, such as a turbine, to be found. These vary in computational intensity, from simple models in which the body is represented as a source or sink, to complicated methods in which the rotor blades and trailing and shed vortices are represented individually by a collection of sources or point vortices. In the modelling of the near wake, potential flow methods can be used to represent rotational effects and vortices caused by the rotor geometry and operating state, without the need for a full, computationally-expensive CFD rotor model. However, in the far wake the effects of the exact rotor characteristics are negligible, and the wake develops through turbulent mixing with the ambient flow. As potential flow is inviscid, turbulent mixing can not be modelled.

3.3 Simplified Computational Fluid Dynamics (CFD) Models

A computational fluid dynamics (CFD) code computes the solution to the Navier-Stokes equations for a flow around a specified geometry at each point within the specified domain. Unlike the Jensen model, the entire flow field has to be calculated to obtain the velocity deficit at the furthest point downstream. In order to analyse the velocity field in horizontal-axis turbine arrays, many rationalised CFD models have been proposed. These have become widely used in the wind energy sector, providing reasonably accurate results without the need for powerful computing equipment.

Early models assumed axial symmetry, such as that proposed by Sforza et al. (1981) which used a linearised momentum equation in the main flow direction, simplified with a constant advective velocity and constant eddy diffusivity (a coefficient for the rate of mixing due to eddies in turbulent flow). The model was first evaluated in two-dimensions, giving suitable wake velocity profiles, before being extended to a three-dimensional model which approximated experimental data with a reasonable degree of accuracy.

Ainslie (1988) first proposed the parabolic field model EVMOD (Eddy Viscosity Model) which still forms the basis of the majority of industrial software packages for wind farm design, such as GH WindFarmer (2010). Ainslie developed a number of empirical formulae from experimental data. Combining these with CFD Navier Stokes calculations, the model gives an accurate solution at a low computational cost. Pressure terms are neglected as the model begins at two diameters downstream, where pressure gradients no longer dominate the flow. A Gaussian profile is applied at this initial point, with the wake width calculated using the momentum integral. Axial symmetry is assumed once again, but an eddy viscosity method based on Prandtl's free shear layer model is implemented for turbulence closure. A comprehensive study was undertaken by Hassan (1993), which allowed systematic validation of Ainslie's approach.

To better represent the effects of an ambient shear layer, Crespo et al. (1988) developed the UPMWAKE model. The turbine wake is no longer modelled as axi-symmetric and a non-uniform basic flow representing the atmospheric boundary layer is assumed. The incident flow over the turbine is predicted using the atmospheric stability, given by the Monin-

Obukhov length, and the surface roughness. A $k-\epsilon$ model is employed for turbulence closure. The model is three dimensional, and requires the SIMPLE algorithm (Versteeg et al., 2007) to solve the combined pressure and velocity fields. The added complexities of the UPMWAKE model make it significantly more computationally-demanding than the Ainslie or Jensen methods. Validation of the techniques used is provided in Crespo et al. (1999).

For the modelling of the entire wake, Voutsinas et al. (1992) proposed a model (later developed by Cleijne et al. (1993)) which applies a different method to each region. A vortex particle method is applied to the rotor region, a simplified CFD method for the near wake and a kinematic-type model for the far wake. This approach reduces computational time by applying suitable assumptions to each area of the wake separately and has been shown to give fair results when compared to experimental data.

3.4 CFD models (Navier-Stokes solvers)

A full CFD model makes fewer assumptions than the simplified models in the previous section. Although codes can be custom built, the majority of analyses to-date have been carried out using commercial software (e.g. Ansys CFX). These offer an integrated selection of algorithms and modelling methods which can be quickly applied by the user. However, a good understanding of the techniques in use is still a necessity if a meaningful model is to be produced. Commercial codes often differ in the methods they support for solving equations, the geometries of meshes employed and the models used to represent turbulence.

The complexity of set-up, difficulties dealing with turbulent flow and high computational demands of a full scale CFD code have led to limited use in far wake analysis. The majority of the turbine models in existence are for the investigation of specific rotor geometries. There are however several research papers which attempt to analyse the far wake and small array layouts using CFD.

As an example, the 3-d CFD model produced by Bai et al. (2009) using the commercial ANSYS FLUENT software is outlined. Tidal turbines were modelled in a grid of 450,000 elements as 20m diameter porous discs (for actuator disc methods, see WG3WP4 D2 – “Near Wake Modelling Report”), which is judged to be sufficient for far wake analysis. In order to reduce computational time, each turbine is modelled only from the centreline upwards, and the result mirrored on the underside of the centreline. Boundary layer effects are therefore neglected. Unfortunately there is no comparison with experimental data to prove the validity of the results. The model does however demonstrate to an extent the interactions between wakes provided by a full CFD model. This can be seen in Figure 3.1, where the highest velocity flow is shown in red and the slowest in blue. Simplified CFD and kinematic models typically use an assumed initial velocity deficit profile, and hence require a second model for the interaction of multiple wakes.

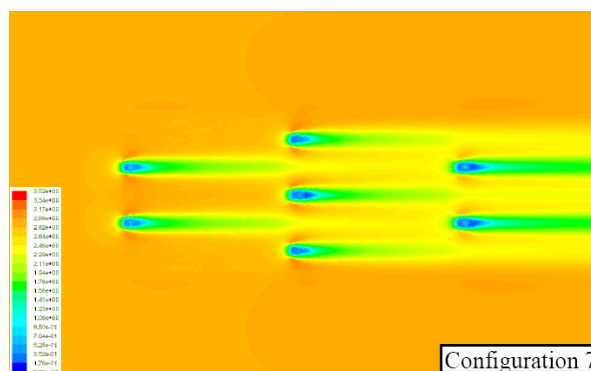


Figure 3-1: CFD representation of a tidal turbine array layout from above. Reproduced from Bai et al. (2009)

3.5 Added turbulence intensity modelling

In addition to a velocity deficit, increased turbulence is a key parameter which can impact on downstream turbines. From a loading analysis perspective, the increased turbulence in the flow can cause additional fatiguing on the device and ultimately shorten its life. Clearly this is undesirable, and thus it is important to accurately evaluate added turbulence effects from upstream turbines on downstream turbines. Within the wind industry, empirical models are employed to model the propagation of increased turbulence in a wake. Although CFD models can provide calculations of turbulence in the wake, these models often employ a Reynolds Averaged Navier Stokes (RANS) turbulence model which tunes the solver to best match the velocity deficit profiles. However, due to the averaging techniques used, this limits the ability to also calibrate the solver to match turbulence characteristics in the flow. The advancement of large-eddy simulation (LES) does, however, provide an opportunity to better couple the solutions of the mean velocity flow field and turbulent flow structures. As the name suggests, LES better models the evolution of large turbulence structures such as wakes.

3.6 Array Modelling

Of key significance when modelling the far wakes of turbines is the impact of the slower moving turbulent flow on downstream devices in a wind or tidal farm. For most simplified CFD and kinematic models, a second model is employed to represent the superposition of wakes. This deals with the three different interactions possible between wakes, as documented by Palm (2009):

- A downstream turbine is placed entirely within the wake of an upstream device
- The wakes behind two adjacent turbines overlap
- A downstream turbine is operating partially in the wake of an upstream device, but partly in the free-stream.

The early model produced by Lissaman combined wakes using a linear superposition method. However, velocity deficits were overestimated, and the combination of many wakes could eventually lead to the unrealistic result of negative velocities. A better model, PARK, was devised by Katic et al. (1986) who linearly superimposed the squares of the velocity deficits. The cumulative deficit in the event of multiple wakes is smaller using this method, and the results usually more accurate.

In GH WindFarmer (2010), Ainslie's method is used for the calculation of individual wake velocity deficits. For each downstream turbine that falls inside a wake, the velocity profile is calculated assuming a Gaussian profile based on the centre line velocity at that distance downstream. If some of a rotor is outside the wake, then the wind speed for that portion of the rotor is set equal to the incident wind speed of the turbine creating the wake. The velocity

profile across the turbine rotor at the hub height is integrated to produce a mean wind speed incident across the rotor at the hub height. This is assumed to represent the incident wind speed across the whole rotor disc.

UPMPARK, developed by Crespo et al. (1994), extends the UPMWAKE code to solve for an array of devices. The software models each turbine as a momentum sink and makes no assumptions about wake superposition effects, hence no wake interaction model is required.

As with UPMPARK, full CFD models do not require a separate technique for the modelling of multiple turbines and wakes. However, the computational demands of the method limit its use for the energy analysis of large arrays. Ivanell (2009) produced a CFD model for the analysis of Horns Rev offshore wind farm off the Danish coast. Even when using a simple actuator disc approach the computation of all turbines in the farm could not be handled, with only 20 of the 80 devices being simulated.

3.7 Summary of relevant modelling methods

An overview of four different modelling methodologies has been presented, and a summary of these is given in Table 3.1. At the most basic level, kinematic models can give a rough solution with minimal effort and understanding. However, wake effects are not calculated with any scientific basis. Potential flow methods assume inviscid fluid behaviour, so cannot represent the turbulent mixing which is required for far wake modelling. Rationalised CFD methods offer a satisfactory compromise between accuracy and computational cost for modelling large arrays. Full CFD models are the most detailed and require fewer assumptions to obtain a solution, but the added complexity increases computation time and the risk of introducing erroneous results via poorly posed boundary conditions and incorrectly selected turbulence closure models. The use of full CFD is relevant at the validation stage, i.e. for a detailed analysis of the optimised array layout, but it is not suitable for use at the design stage due to the computational requirements.

Table 3-1: Summary table comparing modelling methodologies

Model Type	Advantage	Disadvantage
Kinematic	Solution can be found quickly.	Models show only a vague similarity to real system. Simplifications lead to inaccurate solutions for velocity field
Potential Flow	For the near wake the fluid behaviour around the rotor can be modelled without requiring complex CFD calculations.	The inviscid assumption makes it ill-suited for far wake analysis.
Simplified CFD	Good trade off between accuracy and computational requirements. Proven in the wind industry – results correlate well to experimental data.	Unsteady flow and rotor effects are often neglected. The empirical relationships used only hold in situations similar to those for which they were originally developed.
Full CFD	Can represent unsteady flow, rotor effects and wake interactions more realistically.	Very sensitive to exact set-up (selection of appropriate methods is vital). Even with powerful computing resources calculating solutions can take a long time. Limited application in large array analysis.

Increasingly complicated CFD models are now feasible in the analysis of small turbine arrays with a small number of ambient flow speeds and directions. However, in a true wind or tidal farm optimisation exercise, it is not uncommon to model tens of turbines in an array. To make an informed judgement on optimal device layouts many permutations of flow speeds and directions must be considered; GH WindFarmer typically analyses a wind farm for 7200 different flow speed and direction scenarios when performing a full energy assessment. The computational time required to process a full CFD calculation for a large array in this manner would be vast, restricting its use for layout analysis. In such situations, a rationalised CFD approach is preferred, TidalFarmer will therefore use the form of the semi-empirical model developed by Ainslie (1988). The theory behind this model and how it has been and will be adapted in the development of TidalFarmer is discussed in the subsequent sections.

3.8 Review of relevant experimental work

To date there are no (publically-available) full scale measurements of near or far tidal turbine wakes. The authors were previously involved in an experimental testing programme of tidal turbines (Technology Strategy Board (TSB), 2005), summarised in papers by Myers et al. (2008) and Bahaj et al. (2007), which is discussed in detail in Section 7. A review of the literature again reveals that the most applicable set of experiments that have been conducted to date have been in the wind energy sector (further details are given in WG3WP4 D2 – “near wake modelling report”).

4 THE GH FAR WAKE MODEL

This section introduces the GH far wake modelling method and the reasoning behind it. The purpose of the GH far wake modelling is to predict the change in wake form as the wake evolves at different downstream locations. This incorporates both the velocity deficit recovery and the evolution of the wake induced added turbulence.

4.1 GH modelling philosophy

GH's modelling philosophy is to provide engineering solutions to meet a commercial need, and in the case of tidal array design this means providing a design tool that can offer practical solutions to aid the iterative design process. To develop an appropriate design tool, rationalised modelling methods based on a physical understanding of the Navier-Stokes equations that provide robust estimates with known uncertainties are preferred to more complex numerical methods.

4.2 Description of the GH far wake model

The GH far wake model uses a simplified form of the Navier-Stokes equations to model the recovery of a wake in the far field. This model is based on a fundamental understanding of the hydrodynamics of rotors as they extract momentum from the flow and flow dynamics, coupled with experimental tidal and operational wind turbine wake data.

The GH far wake model is a collective of several different models which when combined evaluate the wake development and recovery of multiple turbine wakes within the array. The reduced Navier-Stokes model solvers for a single wake downstream of a turbine, which when coupled with a momentum integral allows the wake at each downstream location to be evaluated. To incorporate the effect of wake merging, several models are available. In addition to evaluating the velocity deficit in the wake the increased turbulence intensity generated by the wakes is also modelled.

The GH far wake modelling incorporates the effect of several key parameters:

- Initial conditions (obtained from the near wake model – as a function of the turbine operating state)
- Ambient flow conditions
 - Ambient turbulence intensity depth profile
 - Flow shear depth profile
- Bounding effects from the seabed, free-surface and other turbine wakes.
- Interaction with other turbine wakes

A detailed description of the theory behind the model is given in Section 5 which further explains how the parameters listed above are incorporated into the model.

The work planned under the PerAWaT project will extend the GH far wake model by developing the wake interaction models and providing further evidence of the impact of ambient turbulence intensity on the wake recovery process. Details of the planned developments are outlined in Section 7.2.

As stated above, CFD is typically used at the validation stage of a design or when better understanding of complex fluid/structure interaction is required. To optimise an array layout, both in terms of maximising energy yield and minimising the loading imparted upon downstream rotors, the inter-array flow field for numerous (10-100s) layout configurations needs to be evaluated. Using CFD to calculate the required flow fields for every layout

would be very computationally expensive and is thus considered not feasible as an engineering tool for array layout optimisation.

The objective of far wake modelling for use in an array tool is to provide a computationally-efficient method for evaluating the altered array flow fields. The derivation of the flow field solution needs to balance accuracy and computational requirements and thus the use of a simplified approach which solves the axi-symmetric problem coupled to interaction models is justified.

5 GH FAR WAKE MODEL THEORY

The GH far wake model is a collection of method and models focused around an eddy-viscosity wake model. Collectively the far wake model includes:

1. An eddy-viscosity model which is the primary flow solver used to evaluate velocity deficit for a single axi-symmetric wake.
2. A momentum integral model: allows for the conservation of momentum within the flow in and around a wake and prescribes the shape of a single wake at each downstream location.
3. Wake interaction models: to incorporate the effect of one wake upon another a selection of wake merging models are available.
4. An added turbulence intensity wake model: is used to predict increased turbulence intensity incident on downstream rotors.

The theory associated with each of these models is described in the section below.

Previous research by Myers et al. (2008) suggests that the wake form (in terms of recovery rates and shape) in an unbounded flow is similar to those seen in the wind industry (for the same levels of ambient turbulence) and that an eddy-viscosity model can be used. However, the validity of using an adjusted axi-symmetric eddy viscosity model to model closely-spaced devices must be considered. The main differences to consider are:

- Different flow unsteadiness and turbulence structures, such as large eddy forms and free-surface waves action, which may impact the wake form and its development.
- The position of the wake within the boundary layer, which may lead to significant differences in flow above and below the wake.
- The presence and proximity of bounding surfaces, which may lead to a limitation of surrounding momentum to feed the wake recovery process

The first point will be addressed via the experimental and numerical investigations and it is expected that the impact of the ambient turbulence intensity value will be adjusted to incorporate these effects. The second point is to a degree addressed in the existing model by the normalisation of the inflow profile. The presence of the bounding surfaces breaks the axi-symmetric assumption. To account for both the asymmetric bounding and flow profile effects, without developing a 3-d numerical model, correction factors to the axi-symmetric solution are proposed by reviewing the available surrounding momentum and limiting wake expansion within the physical flow domain.

5.1 The Eddy Viscosity wake model

The eddy viscosity wake model is a calculation of the velocity deficit field using a finite-difference solution to the thin shear layer equation of the Navier-Stokes equations in axi-symmetric co-ordinates. An illustration of the wake profile used in the eddy viscosity model is shown in the figure below.

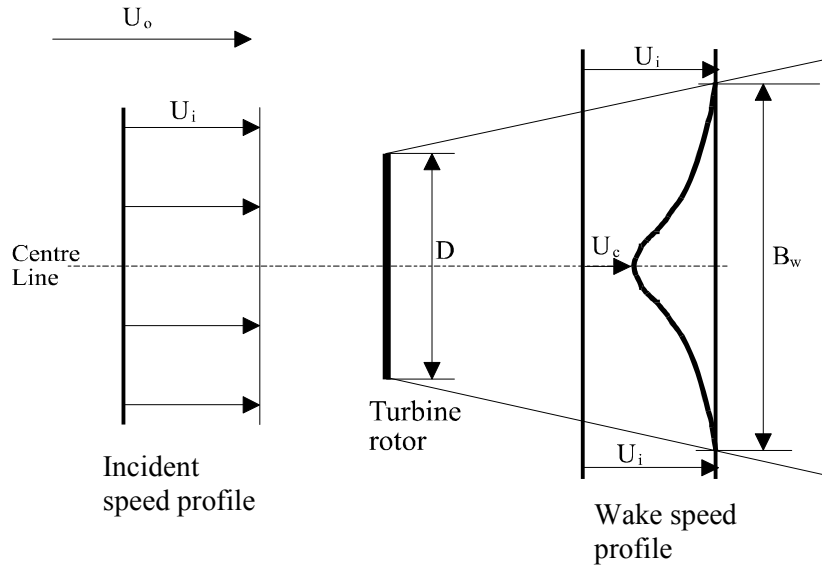


Figure 5-1: Wake profile used in the eddy viscosity model

The axi-symmetric Navier-Stokes equations with Reynolds stresses and the viscous terms neglected in cylindrical coordinates yields:

$$U \frac{\partial U}{\partial x} + V \frac{\partial U}{\partial r} = \frac{-1}{r} \frac{\partial(\overline{ruv})}{\partial r} \quad (5.1)$$

Coupled with the continuity equation, in cylindrical coordinates:

$$\frac{\partial U}{\partial x} + \frac{1}{r} \left(r \frac{\partial V}{\partial r} + V \right) = 0 \quad (5.2)$$

The turbulent viscosity concept is used to describe the shear stresses with an eddy viscosity defined by:

$$\varepsilon(x) = L_m(x) \cdot U_m(x) \quad (5.3)$$

$$\text{and } \overline{-uv} = \varepsilon \frac{\partial U}{\partial r} \quad (5.4)$$

L_m and U_m are suitable length and velocity scales of the turbulence as a function of the downstream distance x but independent of r . The length scale is taken as proportional to the wake width B_w and the velocity scale is proportional to the difference $U_i - U_c$ across the shear layer.

Equation 5.4 permits the shear stress terms \overline{uv} to be expressed in terms of the eddy viscosity.

The governing differential equation to be solved becomes:

$$U \frac{\partial U}{\partial x} + V \frac{\partial U}{\partial r} = \frac{\varepsilon}{r} \frac{\partial(r \partial U / \partial r)}{\partial r} \quad (5.5)$$

The ambient flow for a tidal stream farm it be considered as turbulent, therefore the eddy viscosity in the wake cannot be wholly described by the shear contribution and an ambient term is required. Hence the overall eddy viscosity is given by:

$$\varepsilon = FK_1 B_w (U_i - U_c) + \varepsilon_{amb} \quad (5.6)$$

where the filter function F is a factor applied to correct initial wake conditions and can be introduced to allow for the build up of turbulence on wake mixing. The dimensionless constant K_1 is a constant value over the whole flow field. B_w is the wake width. ε_{amb} is the ambient eddy viscosity and is found using a representative ambient turbulence intensity value. This could be the rotor averaged (or swept area) turbulence intensity or the average turbulence over a multiple of the rotor diameter. Ideally the ambient eddy viscosity is measured directly using site flow measurement equipment to evaluate the ambient flow Reynolds stresses. However, such measurements are costly to obtain and so an empirical relationship based on measured turbulence intensity and atmospheric boundary layer theory is used here in lieu of further evidence. Within the wind industry the ambient eddy viscosity term is calculated by the following equation proposed by Ainslie (1988):

$$\varepsilon_{amb} = K_k^2 I_{amb} / 100 \quad (5.7)$$

K_k is the von Karman constant with a value of 0.4, and I_{amb} is the ambient turbulent intensity. It is the aim of the physical experiments within PerAWaT (WG4WP1&WP2) to investigate the relationship of ambient turbulence intensity and ambient eddy viscosity.

The differential equation (5.5) with the eddy viscosity term (equation (5.6)) substituted in is then discretised using the Crank-Nicolson finite difference method. The constructed tri-diagonal matrix is then solved using a standard numerical method (Press (2002)). The Crank-Nicolson method is based on a central difference in space and the trapezoidal rule in time giving second order convergence in time and is unconditionally stable. The solution for the centreline velocity is then used to further the solution downstream at the next grid node of the wake. The initialisation of the model is provided in part by the near wake model which yields an input flow profile. In addition, the blockage model (WG3WP4D1) can be used to evaluate any local flow changes around the near wake. The device scale modelling report (WG3WP4 D3) describes the method used to establish the velocity field at the beginning of the far wake.

The presence of the two bounding surfaces breaks the axi-symmetry assumption. To account for the asymmetric bounding effects a 3-d model will be required, however, this approach is considered too computationally expensive. An alternative method, developed by GH and based on experimental data, decouples the vertical and lateral conditions to create two models (Myers et al. (2008)). Solving them independently and then combining the solutions for centreline velocity deficit yields a hybrid solution. The lateral model yields the unbounded solution, based on the initial conditions of a bounded disc. The vertical model uses the method of images to reduce momentum entrainment. The vertical model can be further refined to account for the two different vertical boundary conditions. The upper model uses the method of images to reduce momentum entrainment, while the lower model enforces a no-slip boundary condition at the seabed.

It is envisaged that for a row of devices where the lateral spacing is small the available surrounding momentum will be limited and will thus impact the wake recovery. To account for this the model is further split into a left and right lateral model, with bounding effects modelled using the method of images. The boundary conditions for each split model are

derived from the physical location of the various boundaries surrounding the turbine under analysis.

5.2 Momentum integral model

A Gaussian flow speed profile has been shown to be representative of the wake shape in the far wake region (Myers et al. (2008)) and some evidence to support this is presented in Section 7. By applying an integral method it is possible to conserve momentum within the wake allowing the correlation of wake width and centreline deficit. As detailed in the Near Wake Modelling Report (WP3WP4 D2) the following expression for the wake width is obtained:

$$B_w = \sqrt{\frac{3.56_t \times M}{D_m (1 - 0.5D_m)}} \quad (5.8)$$

The wake width B_w used is defined as 1.89 times the half-width of the Gaussian profile, D_m is the centreline deficit and the M is the linear momentum deficit in the wake.

From the solution of wake centreline flow speed and wake width at each axial centreline node the shape and form of the wake at each downstream position can be determined using an elliptical Gaussian profile. An elliptical profile allows vertical wake width to be limited by the water depth. The elliptical characteristics in the far wake model are derived from the physical boundaries at each location in the wake (a full derivation of the elliptical Gaussian profile is provided in Appendix 1 of the Near Wake Modelling Report, WP3WP4 D2). The figure below illustrates the elliptical Gaussian profile.

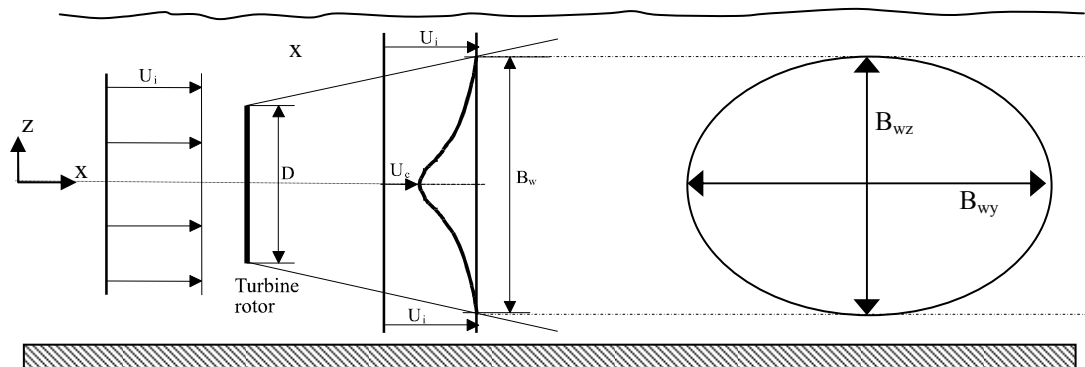


Figure 5-2: Elliptical Gaussian wake model

The elliptical shape shown in the above figure is a first approximation of the wake based on the experimental evidence illustrated in Figure 7-6 (Section 7.1). Despite the different boundary conditions at the bottom and the free surface, the evidence demonstrates that this is a reasonable initial approximation.

The asymmetrical boundary conditions, and therefore the different flow speeds above and below the wake, have the effect of ‘pushing’ the wake centreline lower in the water column, although the shape can still be described as an ellipse. This can be seen in Figure 7-6. Further information is required to more accurately characterise the shape of the wake, and it is anticipated that the results of the CFD and experimental work in WG3WP1, WG3WP5, WG4WP1 and WG4WP3 will provide the necessary evidence to further develop this theory.

As the vertical wake width becomes constrained the lateral wake width increases (using the equation below) to maintain momentum deficit.

$$B_{wy} = \frac{B_w^2}{B_{wz}} \quad (5.9)$$

This approach can be further developed to incorporate other geometric shapes, such as ovals, where the unbounded side of a wake continues to expand whilst the other bounded sides are constrained. Extensions to this approach will be reviewed on the basis of experimental data obtained in WG4WP2.

5.3 Wake interaction models

For each downstream turbine that falls completely inside of an upstream wake, the rotor averaged incident flow speed is calculated and used to evaluate the operating state and thus initial conditions for the downstream turbine wake. Similarly for downstream turbines which experience partial wake submergence, the velocity profile across the turbine rotor is integrated to produce a mean flow speed incident upon the rotor.

To conserve overall momentum within the array a momentum deficit integral centred on the rotor in question is taken at each downstream location. The momentum integral is taken over an elliptic area, which may extend beyond the bounding surfaces or the reflection plane of adjacent turbines. The resulting area averaged momentum is then used to evaluate any correction to the normalised velocity deficit. This allows the eddy-viscosity model to be adjusted at each downstream location, to account for the interaction from an upstream wake.

When two or more wakes overlap, the wakes merge to form a single wake. A number of standard wake merging models have been proposed by Habenicht (2008) and are listed below:

Linear Superposition:	$U_{def,lin} = \sum \left(1 - \frac{U_n}{U_o} \right)$	5.10
Root of the sum of squares (RSS) of velocity deficits:	$U_{def,RSS} = \sqrt{\sum \left(1 - \frac{U_n}{U_o} \right)^2}$	5.11
Average of RSS and linear superposition:	$U_{def} = \frac{U_{def,RSS} + U_{def,lin}}{2}$	5.12
Maximum wake deficit; taking the highest wake deficit to be dominant	$U_{def} = \max \left[\left(1 - \frac{U}{U_o} \right)_n \right]$	5.13

Table 5-1 : Wake merging models

Where U_n represents the axial velocity in the wake from the n^{th} turbine.

The GH approach will be to use the model which provides the closest correlation to the results produced by the physical experiments (WG4WP1, WG4WP2 & WG4WP3) and numerical

simulations (WG3WP2). WG3WP4 D14 (Validation Report on the GH Far Wake Models) will analyse the results of the experimental and numerical test data, and conduct numerical simulations of the far wake models for comparison with the experimental and numerical analysis. The models will then be compared with the validation data set to assess the correlation.

5.4 Semi-empirical added turbulence intensity model

The eddy-viscosity model relies on a value of incident ambient turbulence intensity for calculation of the ambient eddy-viscosity (see equations (5.6)&(5.7)). For a turbine operating outside of another turbine's wake the ambient turbulence level can be used. However, for a turbine operating within another's wake it will be necessary to calculate the increased turbulence level due to wake mixing.

Farm turbulence levels are calculated using an empirical characterisation developed by Quarton and Ainslie (1990) and further developed by Hassan (1993). This characterisation enables the added turbulence in the wake to be defined as a function of ambient turbulence, the turbine thrust coefficient, the distance downstream from the rotor plane and the length of the near wake:

$$I_{\text{add}} = 5.7C_t^{0.7}I_{\text{amb}}^{0.68}\left(x/x_n\right)^{-0.96} \quad (5.14)$$

where x_n is the calculated length of the near wake using the method proposed by Vermeulen et al. (1981).

Using the value of added turbulence and the incident ambient turbulence, the turbulence intensity at any turbine position in the wake can be calculated. Taking an area averaged turbulence intensity in and around a rotor accounts for the rotor not being completely in an upstream wake.

5.5 Summary of the key assumptions

The main assumptions made in the GH far wake model are:

- The wake decay rate in the far wake can be described by an eddy-viscosity model
- The impact of limited surrounding momentum is accounted for using a split modelling approach, where different boundary conditions are imposed to represent both slip and non-slip boundaries.
- The wake shape can be represented by an elliptical Gaussian (or similar) form.
- Wake merging is modelled using a simplified, but standard approach.
- To conserve momentum deficit, checks are made at each downstream location and adjustments made to the velocity deficit.
- Momentum conservation is assumed, in that no net addition of momentum from large scale eddy motion is introduced into the wake region.
- A semi-empirical model is adopted for the assessment of added turbulence intensity in the wake

6 GH FAR WAKE MODEL METHODOLOGY AND IMPLEMENTATION

This section describes how the GH far wake model is incorporated into the TidalFarmer array modelling software tool.

The overall concept of the TidalFarmer modelling method is to reduce the extremely complex interactions between tidal turbines and the surrounding flow field into a distinct physical process which can be simplified and modelled. Classical analysis simplifies the physical process under investigation via the selection of an appropriate scale. The three appropriate scales of interest are Coastal basin, Array and Device scale. The GH far wake model is found at the “Array scale” level.

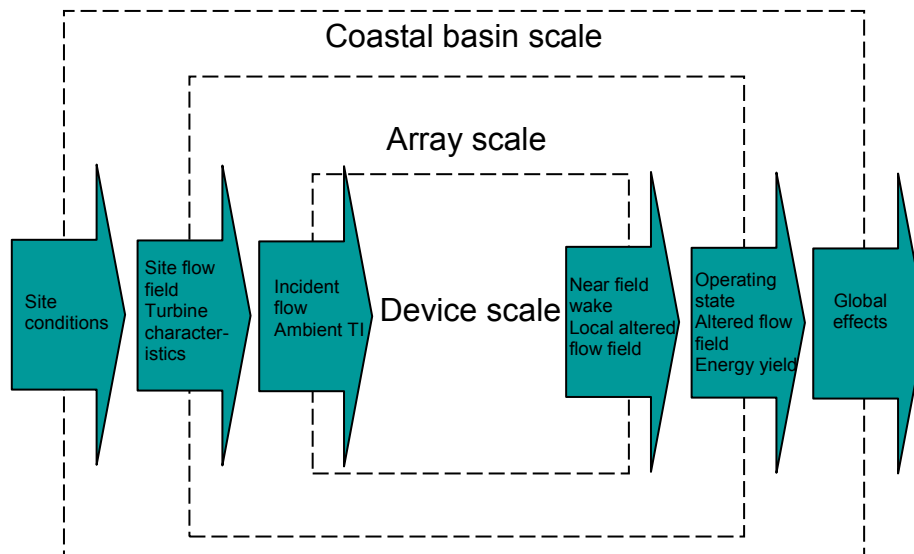


Figure 6-1: Hierarchy of modelling domains and scales

The figure below puts the GH far wake model into context within the TidalFarmer software.

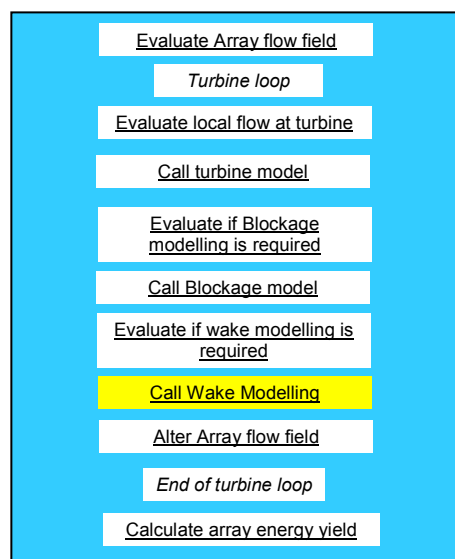


Figure 6-2: Overview of TidalFarmer software architecture showing the GH Wake routine in its context

The GH Wake routine contains both the near wake model and the far wake model. The GH far wake model incorporates several models:

1. Eddy viscosity model
2. Momentum integral model
3. Wake interaction models
4. Added turbulence intensity wake model

The modelling effect of the terrain on the flow is addressed in the rationalised flow field report (WG3WP4D4). The change in flow field due to a wake is addressed in the inter-array scale modelling report (WG3WP4D6) along with the method by which the terrain/wake interactions are accounted for.

The sections below describe how the far wake model is incorporated in to the TidalFarmer software.

6.1 Far wake modelling

To evaluate the far wake flow field due to the recovery of multiple wakes the following set of inputs are used:

- 3-d array flow field (with no turbines)
- For the specific turbine in the turbine loop
 - Local flow field (velocity and ambient turbulence intensity) plane at the rotor location
 - Near wake form (from near wake model)
 - Near velocity field
 - Surrounding momentum in the rotor plane
 - Wake streamline and effective distances to boundaries with other turbines at each downstream location
- Calculation sequence (the order of single wake analysis – dependant on flow direction)

The main core steps are:

For each turbine in the calculation sequence

- Eddy viscosity model
 - Initialise the eddy viscosity solver
 - Evaluate the need for split models
 - Calculate local eddy viscosity parameters and boundary conditions for each of the split models
 - At each downstream grid location
 - For each of the split models solve the finite difference scheme
 - Combine the centreline velocity deficit solutions
 - Momentum Integral model
 - Using the proximity to boundaries (including adjacent wakes) at each downstream grid location evaluate the local wake widths given the centreline deficit and predict the wake form at each downstream location.
 - Assess the surrounding available momentum and correction centreline deficit as required.
 - Adjust Momentum Integral model if required
 - Store altered flow field
- Turbulence intensity wake model
 - The centreline added turbulence intensity at each downstream location

- Use the same elliptical wake form as the velocity deficit

At the end of the each row sequence

- Wake interaction models
 - Evaluate the wake merging from multiple turbines at each downstream grid location.

Update array flow field below looping on next row

Figure 6.3 & 6.4 illustrates the far wake modelling processes and Tables 6.1 and 6.2 provide a functional description of the GH far wake model including reference to the equations presented in Section 5.

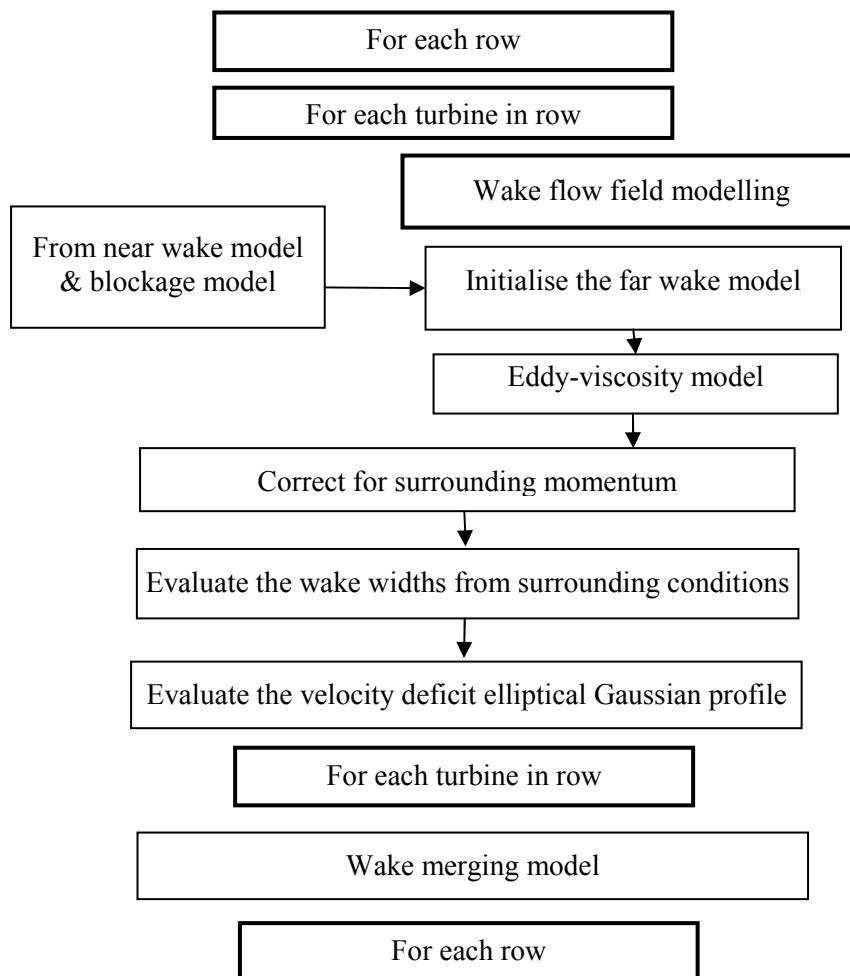


Figure 6-3 Flow diagram of the GH Far wake modelling

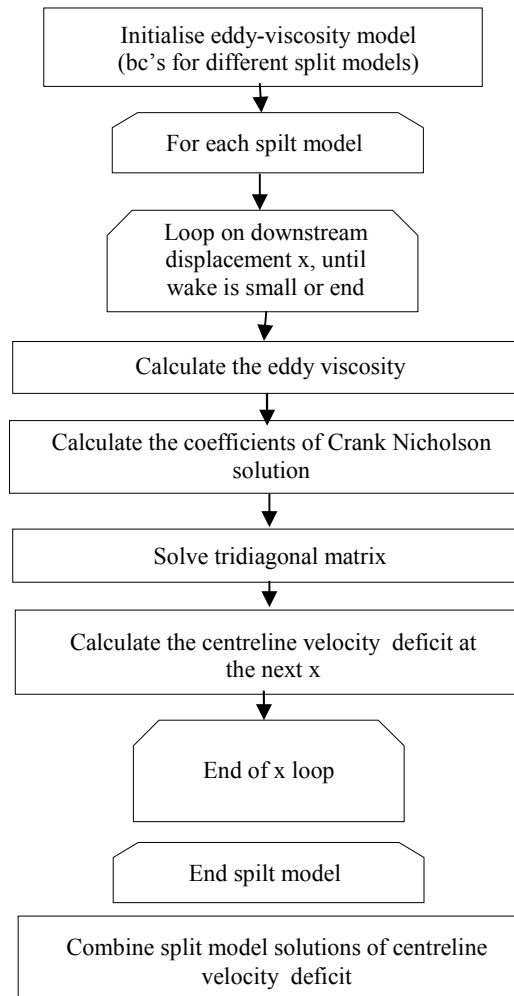


Figure 6-4: Flow diagram of the GH eddy-viscosity wake model

6.2 Implementation

The TidalFarmer software tool will consist of a single user interface with which the user will interact, as well as a number of calculation modules which will be implemented as dynamic-link libraries (DLLs). Tidal calculations will be controlled and coordinated by a top-level “core functionality” module. The GH far wake model will be implemented as part of the wake routine.

Choosing the most appropriate programming language depends on the method of investigation and how the results will be analysed. Currently the code is written as a Matlab script, which allows for easy interrogation and analysis.

The user interface is likely to be written in a .NET language such as C#, while the modules which do the actual calculations will either remain in Matlab or migrate to another language, such as Fortran or C++. The wake-modelling subroutine will be called at the appropriate point in the speed, direction and optimisation loop.

Table 6-1 Summary functional description

Model	Inputs	Outputs	Method used
Eddy viscoisty model	Near wake flow field Array flow field	3-d wake velocity deficit profile at each downstream location	Eddy-viscosity model (Eqn 5.1 to 5.7)
Momentum integral model	Wake centreline deficit Proximity to bounding surfaces	Single wake form at each downstream location	Elliptical Gaussian profile Eqns 5.8 & 5.9
Wake interaction model	Row of single wakes	Merged wakes: updated flow field	One of Eqn 5.10-5.13
Turbulence intensity wake model	Near wake form (ambient turbulence, distance to end of near wake).	Single added turbulence intensity wake at each downstream location	Eqn. 5.14 and Elliptical Gaussian profile derived in the momentum integral

Table 6-2 Detailed functional description of the far wake model

Task	Input	Output	Method
Turbine row loop			
For each turbine in the row loop			
Initialise the eddy viscosity solver			
Proximity assessment	Location of turbine, seabed, hub height, water depth, other local turbines	Distances to local boundaries along wake streamline	Boundary checking algorithm
Calculate local eddy viscosity parameters and boundary conditions for each of the split models	Near wake model outputs Along streamline: Local incident ambient turbulence intensity Distance to local boundaries	Initial and boundary conditions for eddy-viscosity model	Set-up algorithm
At each downstream location			
For each of the split model solve the finite difference scheme	Initial and boundary conditions for each split model	Axi-symmetric velocity field for each model and then the combined velocity field	Crank-Nicoloson discretisation. Numerical solution method. Averaging method
Momentum Integral model	proximity to boundaries the centreline deficit	local wake widths wake form	Elliptical Gaussian profile plus wake width adjustments (Eqns 5.8 & 5.9)
Assess the surrounding available momentum	Local flow field	Correction to centreline deficit as required.	Momentum integral check
Store wake form	Wake form	Updated wake flow field	Matrix allocation algorithm
End downstream location loop			
Turbulence intensity wake model	Near wake model outputs Local ambient turbulence intensity elliptical wake form	Downstream added turbulence intensity wake form	Semi-empirical model (Eqn 5.14).
End turbine in the row loop			
Wake interaction models	Updated wake flow field Selected wake merging model	Updated wake flow field including merged wakes	Evaluate the wake merging from multiple turbines at each downstream grid location using one of Eqns 5.10-5.13
End row loop			

7 VALIDATION

7.1 Existing verification and validation GH far wake model

The authors were previously involved in an experimental testing programme of tidal turbines TSB (2005). The technical outcomes of this project demonstrated that the approach and methodologies adopted were successful in achieving the required quality of results in understanding wake effects (the subsequence figure in this section has been derived from the data acquired during this project). The proposed numerical and experimental modelling techniques were appropriate and have laid the fundamental building blocks for further development. The project identified the following extensions to the work, all of which are being addressed under PerAWaT:

- a) Multiple rotor wake interactions (axially and laterally spaced)
- b) The effect of changing the channel working depth
- c) Better representation of the flow environment

The initial results showed that the fundamental assumption that an eddy-viscosity model coupled with an elliptical Gaussian profile can be used to represent the recovery of a single wake. In addition, the work demonstrated that an elliptical Gaussian distribution could be used to represent the far wake region.

Figure 7.1 shows the general recovery of the wake in the far wake region.

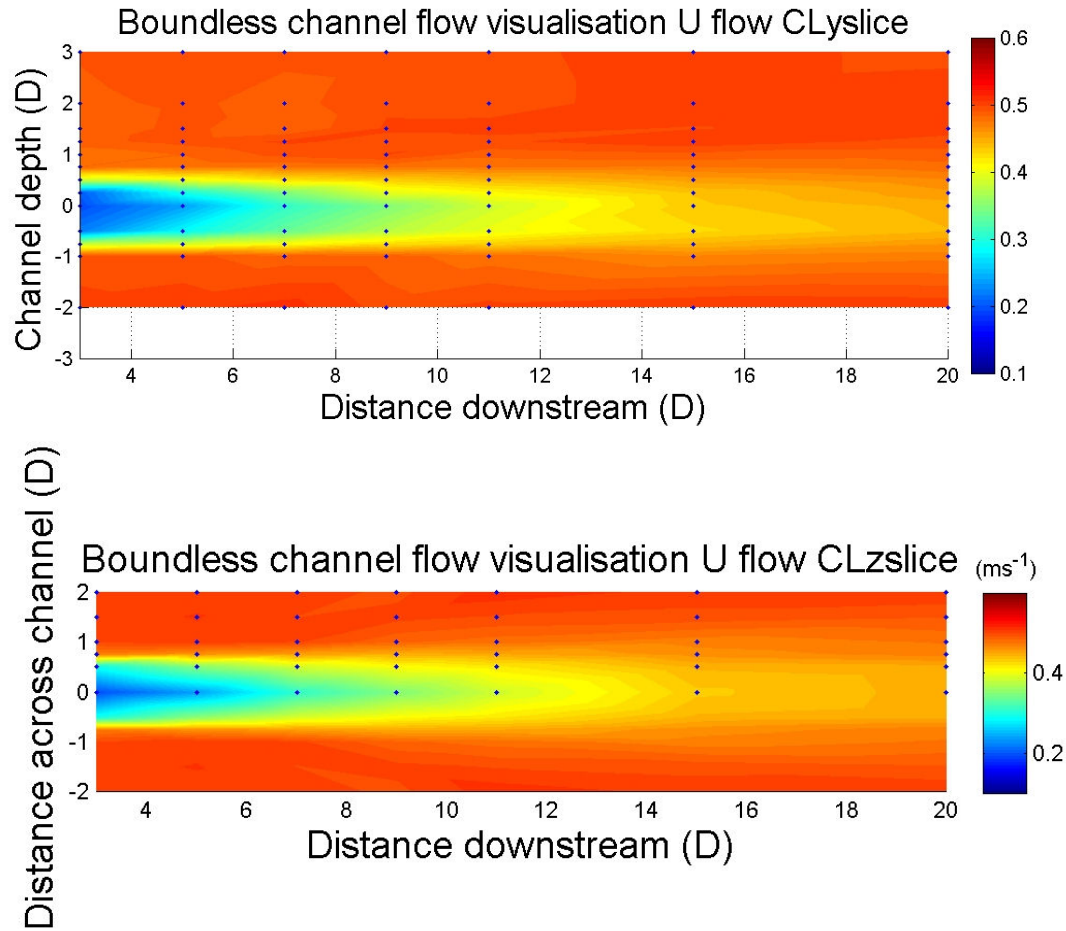


Figure 7-1 Visualisation of the flow field behind a porous disc in a boundless flow (top: slice through the depth at the wake centreline, bottom: slice across the water column at the wake centreline)

To check the fundamental assumption that Reynolds Stresses are driving the wake recovery the data was analysed to yield the relevant Reynolds Stresses. The figure below shows the lateral and vertical Reynolds Stresses (SXY and SXZ respectively) profiles as a function of downstream location. As expected, the Reynolds Stresses increase at the edge of the wake.

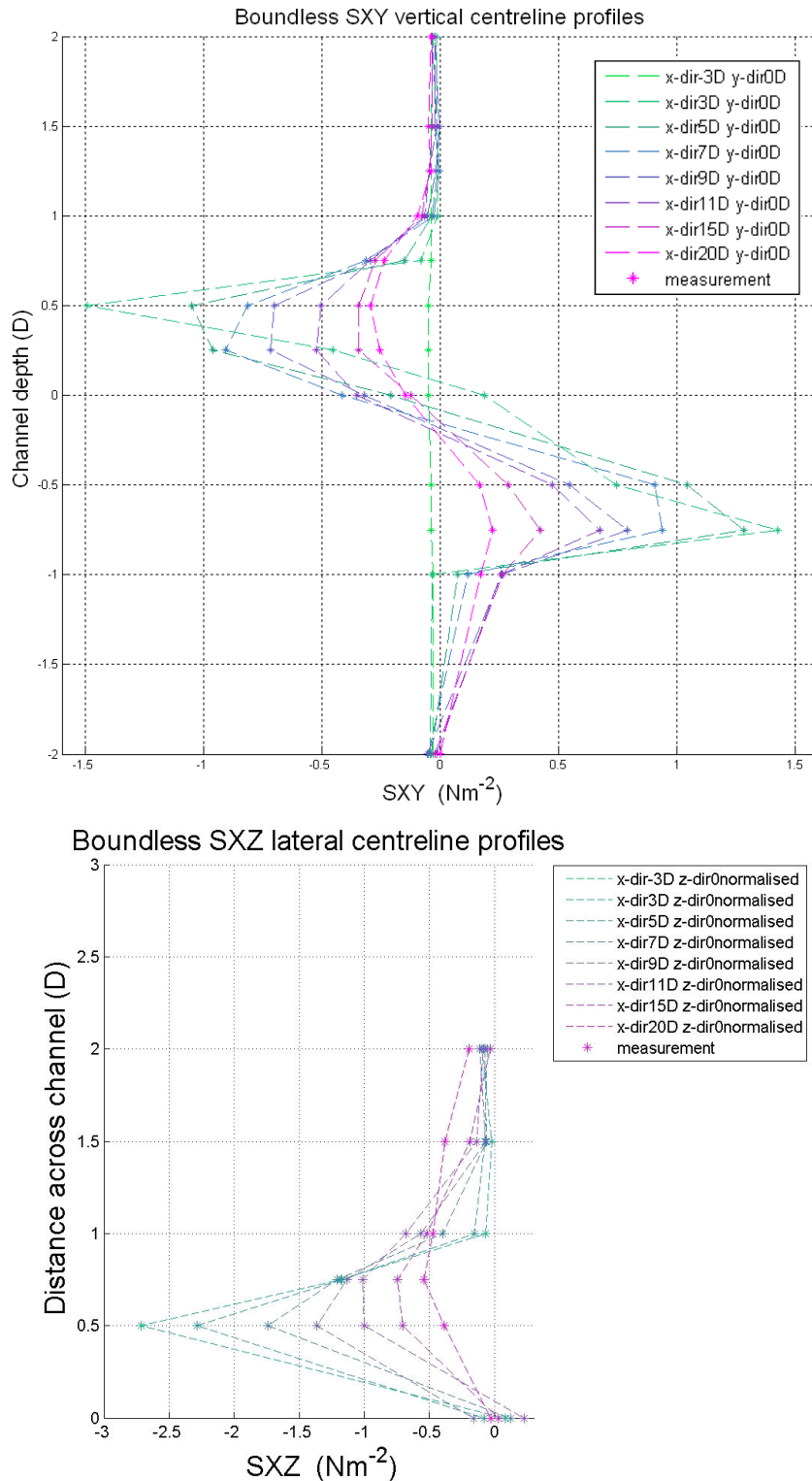


Figure 7-2 Profile plots of the lateral and vertical Reynolds Stresses at different locations downstream of a porous disc in a boundless flow

Using the axi-symmetric eddy-viscosity model for a wake in a boundless flow allows the global parameters to be set. The figure below illustrates the comparison of model and measured Reynolds Stresses.

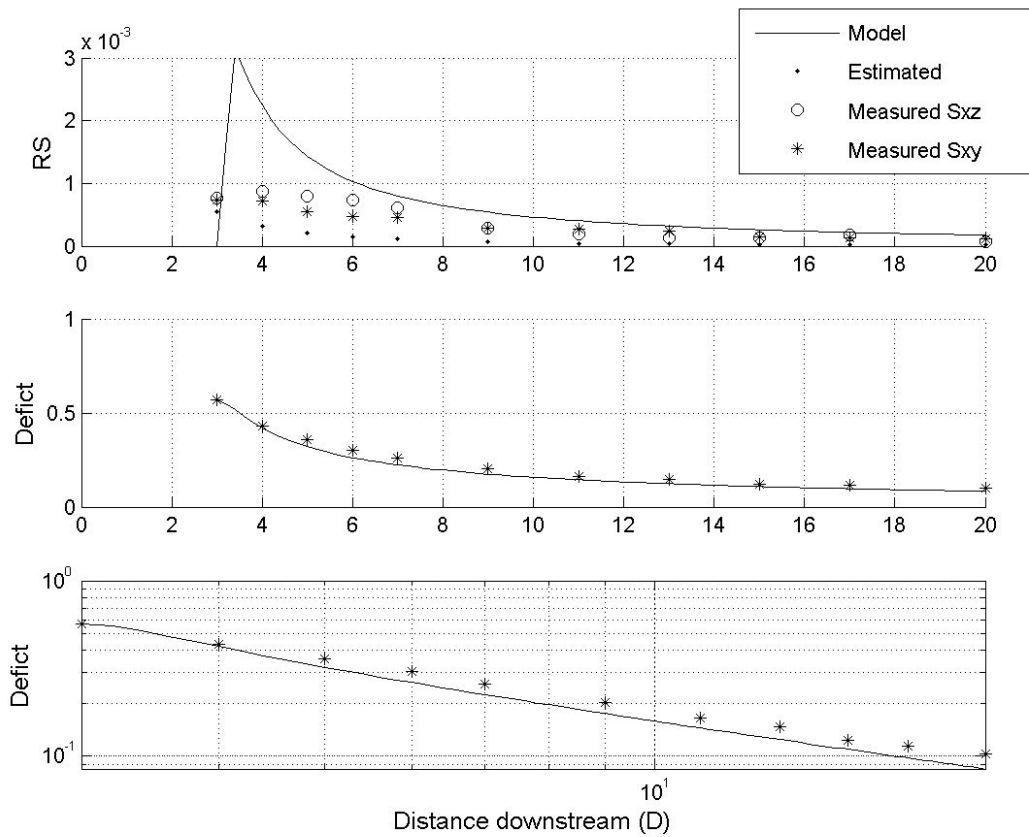


Figure 7-3 Matching the eddy-viscosity model to measured data

As discussed in Section 5 the far wake model uses several solutions of an eddy-viscosity model to incorporate the effect of flow boundaries and a limited amount of surrounding momentum. Figure 7.4 below shows the solutions from the split model as well as comparing the combined solution to measured data.

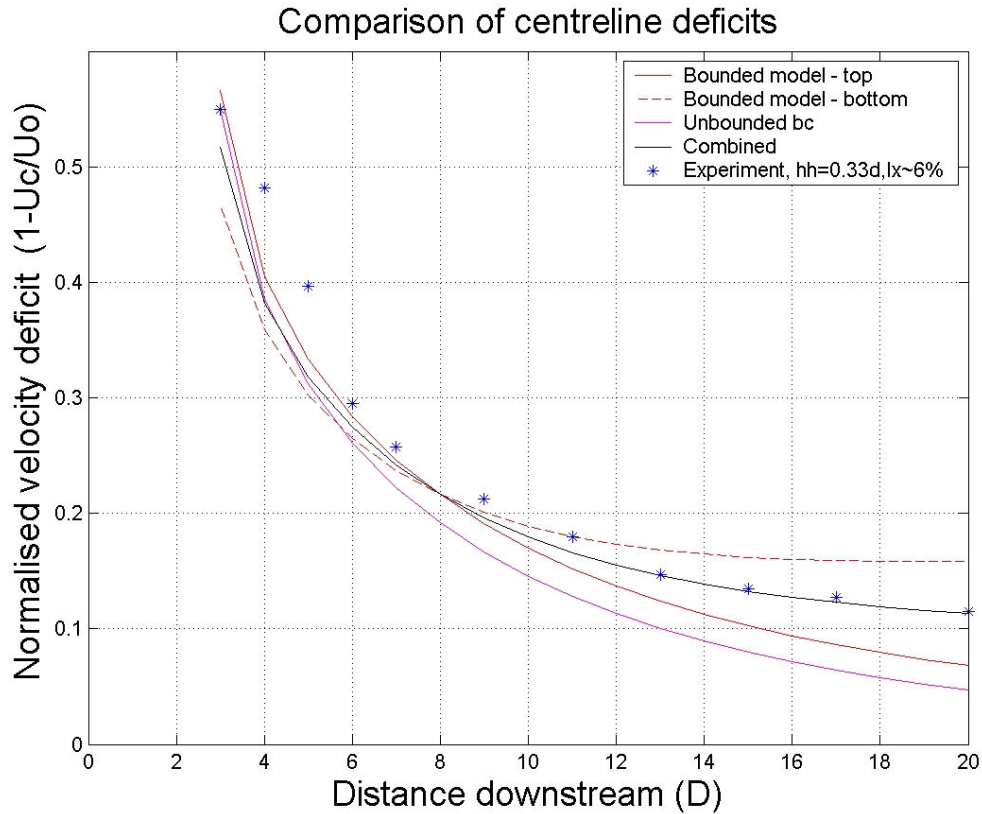


Figure 7-4 Comparison of the split model solutions, the combined model solution and measure data (where the porous disc sits 1/3 of the water depth from the flume floor)

Analysis of the wake profiles at different downstream locations has shown that the Gaussian model yields very similar results to the experimental data (as shown in Figure 7.5 below) providing confidence in the model.

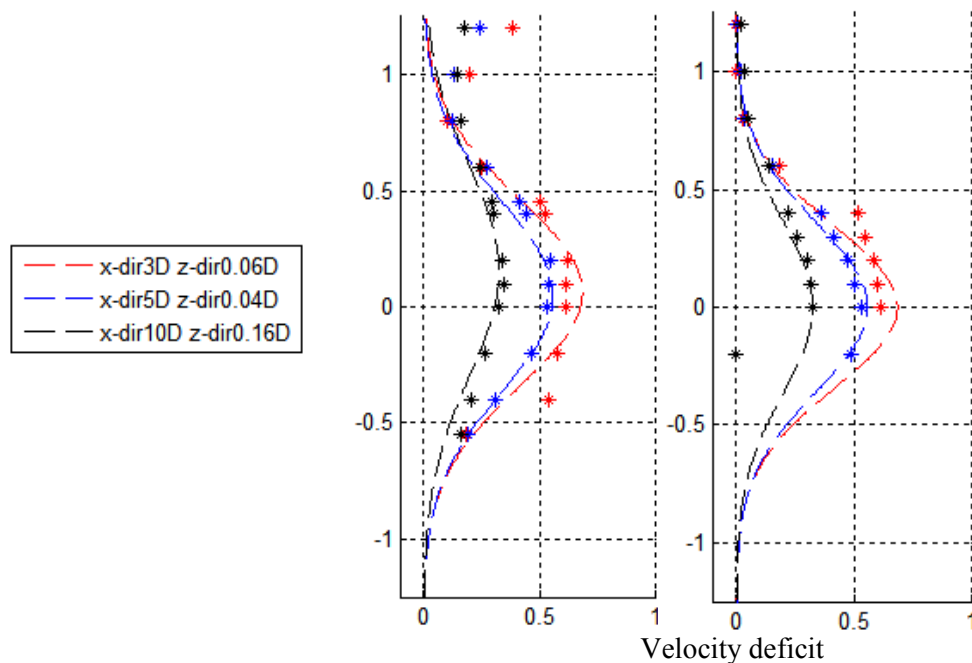


Figure 7-5 Comparison of a Gaussian profile compared to measured data points (left: depth profiles, right: lateral profile, dimensions in rotor diameters).

Figure 7.6 shows the recovery of a wake behind a porous disc and how an elliptical Gaussian profile can be fitted to the data.

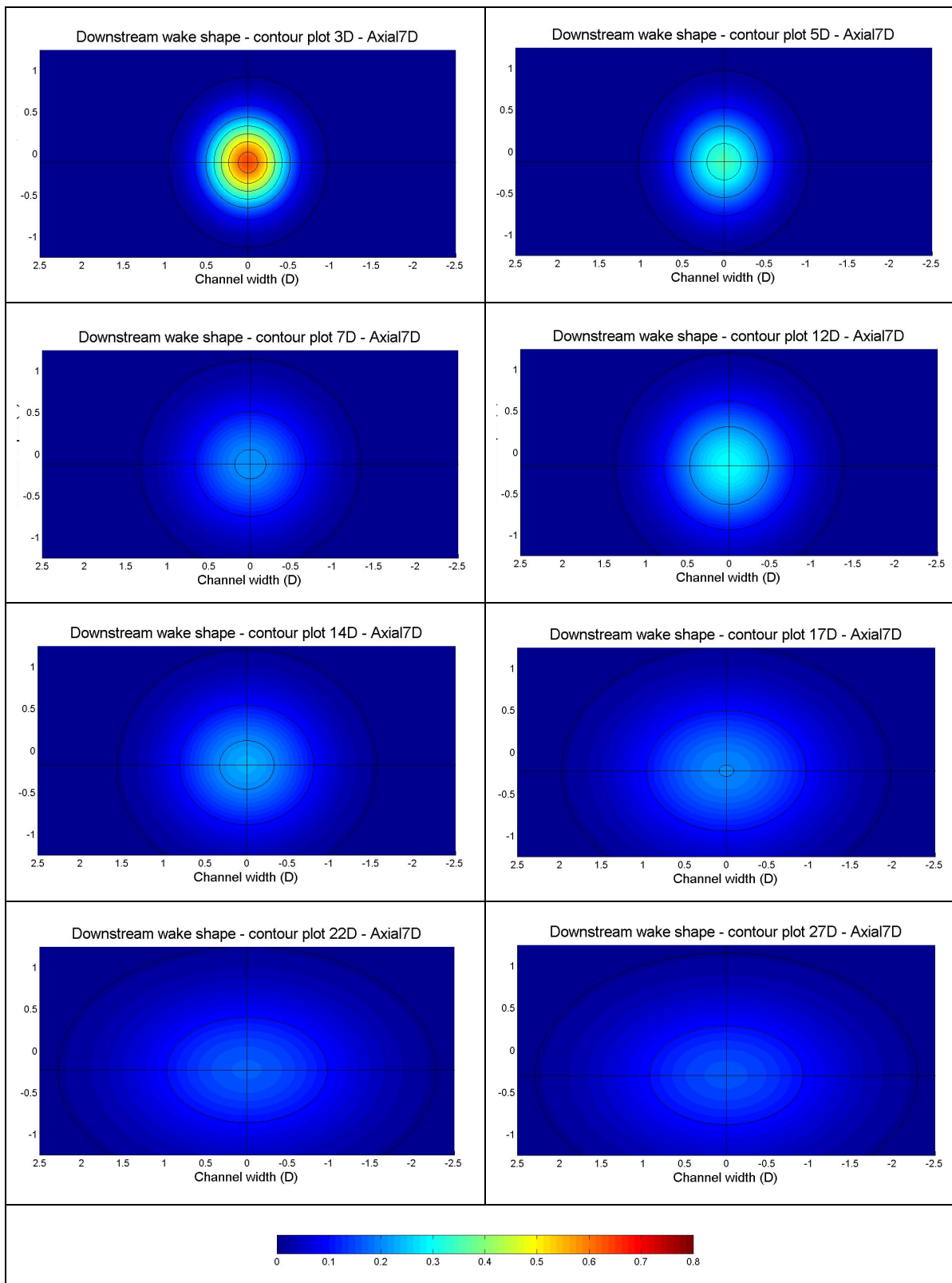


Figure 7-6 Visualisation of measured wake data with an elliptical Gaussian fit (the wake is bounded by a free surface and seabed at $\pm 1.25D$); the colour bar indicates the velocity deficit

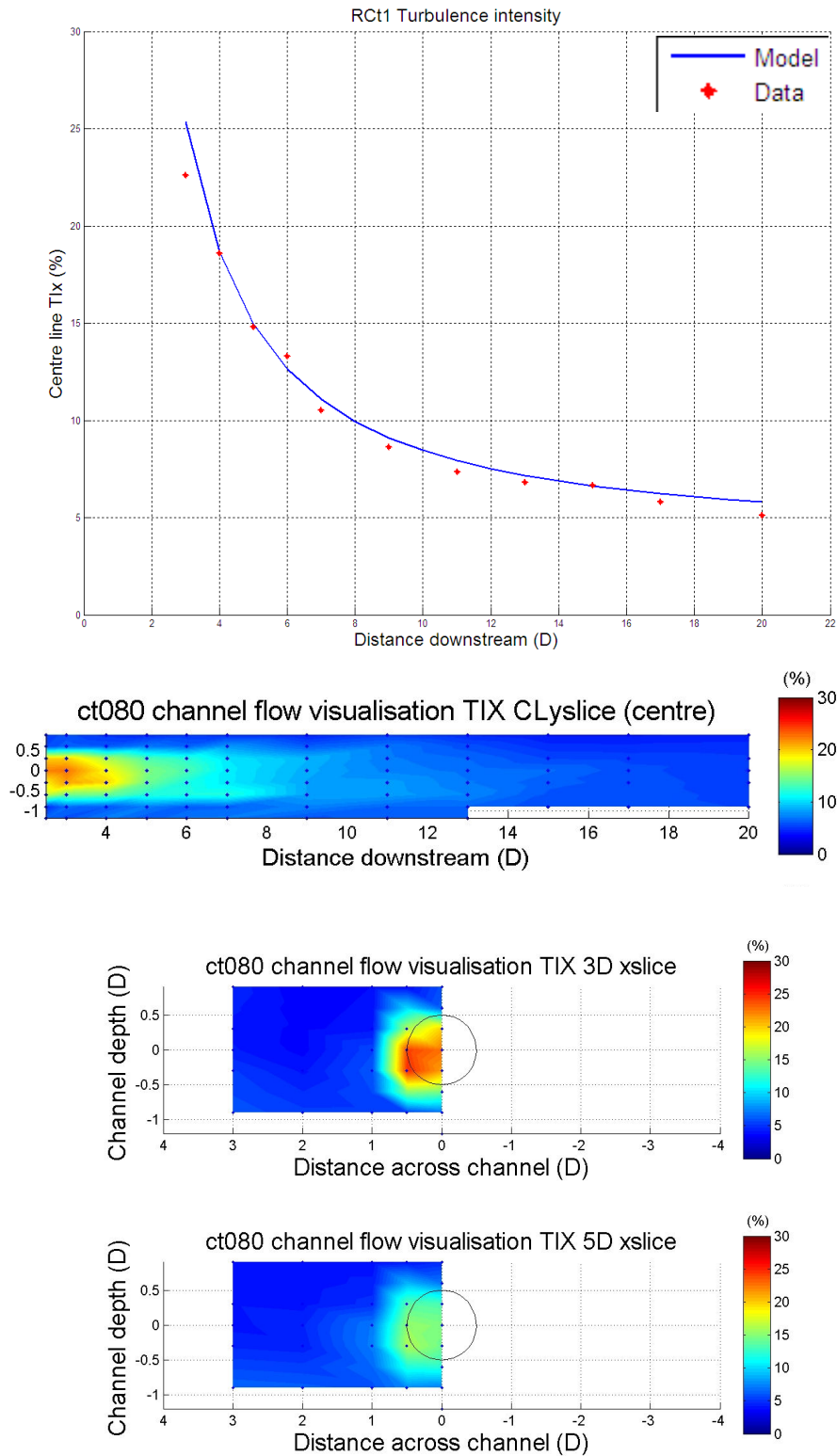


Figure 7-7: Illustrations of the far wake added turbulence intensity model and comparison with rotor wake data

7.2 Developments under PerAWaT

There are several key aspects of investigation in far wake modelling within the PerAWaT project. Evaluating the flow field in the far wake region will be undertaken in a number of work packages via both experimental and numerical investigations. This will provide a dataset for assessing the validity of the developed engineering far wake model.

Experimentally the work packages WG4WP1, WG4WP2 & WG4WP3 all provide measured flow field maps of a single wake from the near wake region and into the far wake. WG4WP1 provides the wake form of a single device operating in different ambient conditions, including varied seabed roughness generated turbulence and wave generated turbulence. WG4WP2 will provide wake maps of multiple devices interacting both laterally and longitudinally, allowing further assessment of the developed spilt model and assessment of different wake merging models. In addition, varied ambient flow conditions will be used to further investigate the impact of ambient turbulence intensity profiles on multiple wake recovery. WG4WP3 will provide device scale wake maps behind open centre and ducted turbines, enabling the impact of near wake profiles to be assessed on far wake modelling.

The PerAWaT work package WG3WP2 will provide CFD simulation results of the far wake region to further demonstrate the effects of the free surface and seabed, as well as closely spaced devices.

Rotor performance and loading data from the ReDAPT (Reliable Data Acquisition Platform for Tidal) project will also be utilised if available. This data will further validate the application of this model for full scale scenarios.

The numerical and physical validation tests will provide a robust set of tests to which the GH far wake model can be compared. The GH far wake model will be set up to be directly analogous with each physical test undertaken in WG4WP2 allowing direct comparison and thus validation of the model. The input parameters for comparison are the base flow conditions (ambient velocity and turbulence intensity fields), rotor thrust and the proximity to boundaries and/or other turbine wakes. The output parameters for comparison will be velocity and turbulence intensity flow field maps and profiles in the far wake region.

One of the main aims of the PerAWaT project is to investigate the appropriateness of using the adapted Ainslie model to represent the wake behind a tidal turbine. This work will establish the impact of the change in flow conditions and the bounding effect of a free surface.

The impact of uncertainty around experimental and numerical results will be investigated to assess the impact on the far wake model uncertainty.

8 SUMMARY

This report describes the GH far wake model, including a literature review of the different modelling techniques. The theory and methodology of the GH far wake model have been detailed and an account of how the model will be incorporated in the TidalFarmer beta code is provided.

The GH far wake model is an arrangement of several models which collectively provide an array far wake modelling method. The eddy-viscosity model is the core flow solver which predicts the recovery of a single wake based on the initial velocity deficit profile and the ambient flow turbulence intensity. A split modelling approach decouples the vertical and lateral boundary conditions allowing a fast computation of several 3-d wakes. By combining the split models a representative wake is evaluated. The model utilises an elliptical Gaussian profile to account for the interaction with the bounding free-surface and seabed.

The selection of the most appropriate wake merging model will be based on the experimental evidence provided in WG4WP2.

The next steps for this work package are:

- to analyse the experimental results provided from WG4WP1, WG4WP2 & WG4WP3
- to issues and support the beta testing of the TidalFarmer code
- to compare the results to the existing model and adjust as required
- to further compare the single far wake model with the numerical modelling results provided from WG3WP1 & WG3WP5
- to analyse and report on the uncertainty associated with the model in WG3WP4 D14.

9 BIBLIOGRAPHY

Ainslie, J. F., “Calculating the flowfield in the wake of wind turbines”, *Journal of Wind Engineering and Industrial Aerodynamics*, 27: 213-224, 1988.

Ainslie, J. F., “Development of an eddy viscosity model for wind turbine wakes”, Central Electricity Research Laboratories, Leatherhead, Surrey. , 7th BWEA Conference Proceedings, Oxford, 1985

Bahaj, A.S., Myers, L.E., Thomson, M.D. & Jorge, N., “Characterising the wake of horizontal axis marine current turbines”, *Proceedings of 7th European Wave and Tidal Energy Conference*, Porto, Portugal, 2007.

Bai, L., Spence, R.R.G., Dudziak, G., “Investigation of the Influence of Array Arrangement and Spacing on Tidal Energy Converter (TEC) Performance using a 3-Dimensional CFD Model”, *Proceedings of the 8th European Wave and Tidal Energy Conference*, Uppsala, Sweden, 2009

Cleijne, J.W., Crespo A, Huberson S, Taylor G.J., Voutsinas S.G. “Wake and wind farm modelling”, Report 93-374, TNO-MT, Apeldoorn, Netherlands, 1993.

Crespo, A, Hernández, J., Fraga, E. & Andreu, C, “Experimental validation of the UPM computer code to calculate wind turbine wakes and comparison with other models”, *Journal of Wind Engineering and Industrial Aerodynamics*, 27, 77-88, 1988.

Crespo, A, Chacón, L., Hernández, J., Manuel, F., & Grau, J., “UPMPARK: a parabolic 3D code to model wind farms”, *Proceeding of the European Wind Energy Conference*, Thessaloniki, 454-459, 1994.

Crespo, A. and Hernández, J. & Frandsen, S. “Survey of modeling methods for wind turbine wakes and wind farms”, *Journal of Wind Energy*, 2: 1-24, 1999.

Garrad Hassan and Partners Ltd. Development of a design tool for axial flow tidal stream devices. BERR document, URN No. 08/852, Contract No. T/06/00231/00/00, 2008.

GH WindFarmer - Theory Manual, version 4.1, Garrad Hassan and Partners Ltd, February 2010.

GH WindFarmer Validation Manual, Garrad Hassan and Partners Ltd, Bristol, UK, 2003.

Habenicht, Gerd, Comparison of different Wake Combination methods for Offshore wake modelling, Dansk Forskningskonsortium for Vindenergi Program, 2008.

Hassan, U., A wind tunnel investigation of the wake structure within small wind turbine farms. Garrad Hassan and Partners, ETSU WN 5113, United Kingdom, 1993.

Ivanell SSA., Numerical computations of wind turbine wakes, Doctoral thesis, KTH, Royal Institute of Technology, Stockholm, 2009

Katic I, Høstrup J and Jensen N, “A simple model for cluster efficiency”, *Proceedings of the BWEA Conference*, 1986.

Lissaman, P.B.S., “Energy effectiveness of arrays of wind energy conversion systems”, Technical report AV FR 7058, AeroVironment Inc., Pasadena, California, USA, 1977.

Lissaman, P.B.S., "Energy effectiveness of arbitrary arrays of wind turbines", *Journal of Energy*, 3(6): 323-328, 1979.

Myers, L.E., Bahaj, A.S., Rawlinson-Smith, R.I., Thomson, M.D., "The effect of boundary proximity upon the wake structure of horizontal axis marine current turbines", *Proceedings of 27th International Conference on Offshore Mechanics and Arctic Engineering*, Estoril, Portugal, 2008.

Myers, L.E., Bahaj, A.S., "Experimental analysis of the flow field around horizontal axis tidal turbines by use of scale mesh disk rotor simulators", *Ocean Engineering*, 37: 218-227, 2010.

Palm, M., "Influence of wakes on tidal turbine performance and farm arrangements", *Master Thesis, Offshore Engineering, Delft University of Technology*, November 2009.

Press, William H., "Numerical Recipes in C++, The art of scientific computing", *Cambridge University Press*, Second Edition, 2002

Quarton, D.C. & Ainslie, A., P.B.S., "Turbulence in wind turbine wakes", *Wind Engineering*, 14(1), 1990.

Sforza, P.M., Sheerin, P. & Smorto, M., "Three-dimensional wakes of simulated wind turbines", *AIAA Journal*, 19(9) 1101-1107, 1981.

Tennekes, H. & Lumley, J.L., *A first course in turbulence*. MIT Press Cambridge, Massachusetts, USA, 1972.

Thake, J., (IT Power), *Development, installation and testing of a large-scale tidal current turbine*. DTI document, URN No. 05/1698, Contract No. T/06/0021/00/REP, 2005.

Technology Strategy Board (GRANT REFERENCE NO. T/06/00241/00/00 (200018) PERFORMANCE CHARACTERISTICS AND OPTIMISATION OF MARINE CURRENT ENERGY CONVERTER ARRAYS), 2005.

Vermeer, L.J., Sorensen, J.N. & Crespo, A., "Wind turbine wake aerodynamics", *Progress in Aerospace Sciences* 39: 467-510, 2003.

Vermeulen P and Vijge J, "Mathematical Modelling of Wake Interaction in Wind Turbine Arrays", report TNO 81-02834, 1981

Versteeg, H. K., Malalasekera, W., "An Introduction to Computational Fluid dynamics: The Finite Volume Method", *Pearson Education Limited*, Second Edition, 2007

Voutsinas S.G., Glekas J.P., Zervos A., "Investigation of the effect of the initial velocity profile on the wake development of a wind turbine", *Journal of Wind Engineering and Industrial Aerodynamics*, 39:293-301, 1992.